Cellulose (2020) 27:3889–3902
https://doi.org/10.1007/s10570-020-03034-8

ORIGINAL RESEARCH

A novel cellulose acetate/poly (ionic liquid) composite air filter

Mengni Zhu · Qiping Cao · Bingyang Liu · Haoyu Guo · Xing Wang · Ying Han · Guangwei Sun · Yao Li · Jinghui Zhou

Received: 31 May 2019 / Accepted: 31 January 2020 / Published online: 10 February 2020

Abstract Global air pollution poses a serious risk to human health. Among the variety of types of pollution, inhalable particulate matter (PM 2.5) is proved to be extremely harmful. In this work, a simple method was designed to synthesize a novel air filter, which composed of cellulose acetate and poly (ionic liquids) by using the technique of macromolecular design and electrostatic spinning process. The introduction of poly (ionic liquids) effectively reduced the diameter of fibers and thus obtains nano-fibrous filters. The removal rate of PM 10 and PM 2.5 particle by the filters reached 99.65% and 97.94%, respectively. Furthermore, the filters exhibited excellent antibacterial properties against *Escherichia coli* and *Staphylococcus aureus*, and no obvious cytotoxicity was observed in vitro culturing cell. After multiple recycling, the filters still maintained excellent antimicrobial properties and fibrous morphology due to the stable covalent bonds between cellulose acetate and poly (ionic liquids). This is a novel strategy to prepare high-quality air filters, which have great potential applications in air purification.

Graphic abstract We fabricated a kind of green electrospinning material with stable antibacterial properties through organic synthesis and molecular design. The introduction of poly (ionic liquids) effectively reduces the diameter of fibers and thus obtains nano-fibrous filters. The removal rate of PM 10 and PM 2.5 particle by the filters reached 99.65% and 97.94%, respectively. Furthermore, the filters exhibit excellent antibacterial properties against E. coli and S. aureus, and no obvious cytotoxicity is observed in vitro culturing cell. After multiple recycling, the filters still maintain excellent antimicrobial properties and fibrous morphology.

Electronic supplementary material The online version of this article (https://doi.org/10.1007/s10570-020-03034-8) contains supplementary material, which is available to authorized users.

M. Zhu · Q. Cao · B. Liu · H. Guo · X. Wang · Y. Han · G. Sun · Y. Li (✉) · J. Zhou (✉)
Liaoning Province Key Laboratory of Pulp and Papermaking Engineering, Dalian Polytechnic University, Dalian, Liaoning Province, China
e-mail: liyaodlpu@163.com

J. Zhou
e-mail: zhoujh@dlpu.edu.cn

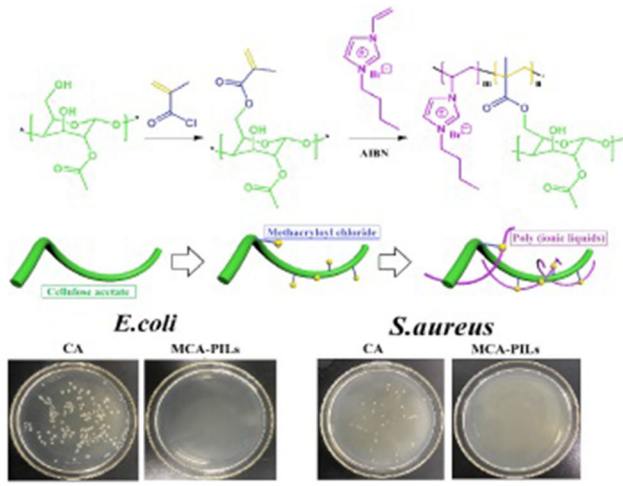

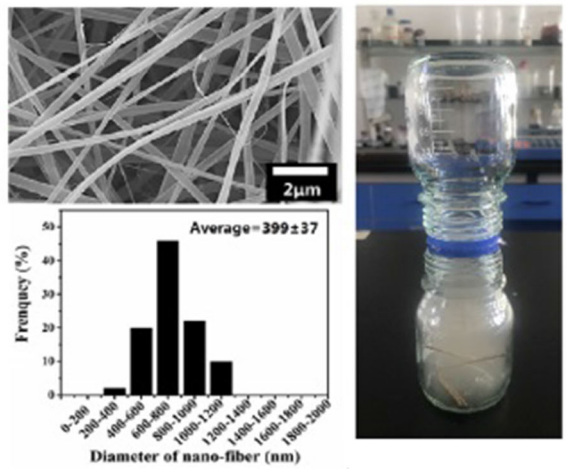

Keywords Cellulose acetate · Poly (ionic liquids) · Molecular design · Nano-fibrous · Air filter and antimicrobial

Introduction

Global air pollution poses a serious risk to human health, climate, and ecosystems (Lu et al. 2017; Fan et al. 2018). Among the variety of types of pollution, particulate matter 2.5 (PM 2.5) (an aerosol particle with an aerodynamic diameter of less than or equal to 2.5 μm) is proved to be extremely harmful, because it is particularly prone to penetrating human lungs (Wang et al. 2014), bronchi and even through the bloodstream (Zhang et al. 2016). Toxicological and epidemiological studies have indicated that long-term exposure to high levels of PM 2.5 pollution result in serious physical diseases, such as respiratory and cardiovascular diseases and even mental functions decline (Brook et al. 2010; Raaschou-Nielsen et al. 2013; Hu et al. 2017). Many effective strategies have been developed and applied to relieve the PM 2.5 pollution, such as improving the material-fuel quality, using better combustion technology to increase the combustion efficiency, and driving down the PM 2.5 emission by vehicle lightweight strategies (Li et al. 2016; Shanmugam et al. 2019). However, these strategies are usually expensive and technically difficult to implement (Jing et al. 2016; Zhang et al. 2019a, b). In addition, it is really long and complex to change the long-term hazy weather that has already became a considerably serious problem in many metropolis like Beijing and Shanghai (Zhu et al. 2018a, b). Therefore, it is an urgent solution to cut the PM 2.5 level of the individual's living environment which could protect them from the PM 2.5 exposure (Zhu et al. 2018a, b)

Filtration is one of common and effective methods for PM 2.5 removal and air purification to improve the individual's living environment (Xiong et al. 2017) Air filters have been widely applied in various applications, including in disposable respirators (Tan et al. 2019), indoor air purification (Khalid et al. 2017; Zhang et al. 2019a, b), industrial gas cleaning (Liu et al. 2018) and automotive engine intake filters (Osaka et al. 2019). Currently, commercial air filters are usually fabricated using microfibers, which have a low air resistance and a maximal capacity of pollutant, but their removal efficiencies of fine particles are usually limited (Wang et al. 2016). To improve filtration efficiency, the electrospun nano-fibers air filter display an excellent performance compared with those of microfibers (Tort and Acarturk 2016; Tan et al. 2019; Zhu et al. 2019). The sinuous and connected channels of nano-fibers are beneficial for the low air resistance and high filtration efficiency, simultaneously (Zhang et al. 2019a, b). Electrostatic spinning is the main method to obtain nano-fibers (Zhu et al. 2017). A viscoelastic polymer and/or biomacromolecule solution with sufficient conductivity can be electrospun into micro- and nanosized diameter fibers by releasing from a spinneret and collecting on a

grounded collector surface (Xue et al. 2019). Based on the electrostatic spinning technology, a large amount of nano-fibers have been prepared for PM 2.5 air filters with high filtration performance (Li et al. 2019; Zhu et al. 2019). However, some polymer-based nano-fibers lack biological compatibility and environmental friendliness (Zhang et al. 2016; Gu et al. 2017; Wang et al. 2018a, b). In addition, air filters are prone to be contaminated by microorganisms after long-term use, which is very negative for human health (Han et al. 2019). In recent years, many strategies are employed to improve antimicrobial ability of air filters, such as mixed antibacterial metals, antibacterial nano-particles and antibacterial polymer (Ma et al. 2018). Among these antimicrobial materials, poly (ionic liquids) materials are potential candidates because of their excellent antimicrobial properties, processability, and flexibility (Wang et al. 2019). The antimicrobial mechanism of poly (ionic liquids) materials is similar to that of natural macromolecule chitosan (Fang et al. 2019). The poly (ionic liquids) materials have numerous active chemical groups with positive charge, which effectively destroy the phospholipid bilayer membrane of bacteria, thereby killing bacteria (Elshaarawy et al. 2019). However, poly (ionic liquids) material with the excellent solubility and hydrophilicity is easily lost in the application process, which makes it impossible to recycle (Cheng et al. 2018). Consequently, it is highly desirable to fabricate air filters with low air resistance (Fan et al. 2018), good biocompatibility (Zhu et al. 2018a, b), environmentally friendly properties (Wang et al. 2018a, b),excellent antimicrobial properties (Zhu et al. 2018a, b), and flexibility for the removal of PM 2.5 (Ma et al. 2019).

Cellulose as the first most abundant natural polymer in the plant cell has received increasing attention for the use in renewable adhesive (Arca et al. 2018), coating (Napso et al. 2018), engineering plastic (Song et al. 2017), and hydrogels (De France et al. 2019).Unique advantages of cellulose, including low cost (Yang et al. 2019), renewability (Sobhanadhas et al. 2019), and environmentally friendly properties (Song et al. 2017), make it an attractive choice as an idea material for air filters (Sobhanadhas et al. 2019). However, cellulose nano-fibers have a low removal efficiency for PM 2.5, which is due to the lack of active chemical groups on the surface of cellulose nano-fibers (Jiang et al. 2013). In this work, we designed a simple method to synthesize a novel air filter, which composed of cellulose acetate and poly (ionic liquids) by using the macromolecular design technique and electrostatic spinning process. The ionic liquids containing olefin group could copolymerize with the modified cellulose to obtain the electrostatic spinning dope. The stable covalent bonds between poly (ionic liquids) and cellulose acetate is beneficial for reduce the loss of the poly (ionic liquids). In the process of electrostatic spinning, the introduction of poly (ionic liquids) could effectively increase the tensile force in electrostatic field, and then the diameter of electrostatic spinning fibers will be further reduced to obtain nano-fibrous filters (Seo et al. 2009; Lopez et al. 2018; Bazbouz et al. 2019). The removal rate of PM 10 and PM 2.5 particle by the filters reached 99.65% and 97.94%, respectively. Furthermore, the filters exhibited excellent antibacterial properties against *E. coli* and *S. aureus*, and no obvious cytotoxicity was observed in vitro culturing cell. After multiple recycling, the filters still maintained excellent antimicrobial properties and fibrous morphology attributed to the stable covalent bonds between cellulose acetate and poly (ionic liquids). This is a novel strategy to prepare high-quality air filters, which have great potential applications in air purification.

Experimental section

Materials

Cellulose acetate (CA) and methacryloyl chloride were purchased from Aladdin Industrial Corporation (Shanghai, China). N, N-dimethylformamide (DMF) and 2, 2′-azobis (isobutyronitrile) (AIBN) were procured from Da Mao Reagent (Tianjin, China). N-butyl bromide was purchased from Shanghai Macklin Biochemical Industry Co., Ltd., China. 1-vinylimidazale was kindly provided by Energy Chemical (Shanghai, China). Ethyl acetate was obtained from Da Mao Reagent (Tianjin, China). Acetic acid was purchased from Tianjin Kermel Chemical Reagent Co., Ltd., China. Both the *E. coli* (ATCC 25922) and *S. aureus* (MCCCB 26003) strains were purchased from Shanghai Luwei Technology Co. Ltd (Shanghai, China). Mouse osteoblast cell line was obtained from the Cell Bank of Type Culture Collection of the Chinese Academy of Sciences (Shanghai, China). All

chemicals were used as received without further purification.

Synthesis of 1-vinyl-3-butylimidazale bromide

The synthetic route for 1-vinyl-3-butylimidazale bromide was shown in the Scheme 1a. 6.85 g n-butyl bromide and 4.70 g 1-vinylimidazale (molar ratio = 1:1) were added to a 10 mL vial and then mixed with 1 mL ethyl acetate. The mixture was magnetically stirred at room temperature for 5 days. Finally, the product 1-vinyl-3-butylimidazale bromide was obtained (yield: 92%).

Synthesis of modified cellulose acetate nano-fibrous filters

The synthetic route for the cellulose acetate modified by poly (ionic liquids) was shown in the Scheme 1b. Cellulose acetate (CA, 4.0 g) and triethylamine (0.4 g) were dissolved in N, N-dimethylformamide (DMF, 30 mL) in a 50 mL three-necked flask under stirring at 80 °C to form a homogenous solution. Then, methacryloyl chloride (0.4 g) with DMF (10 mL) was added dropwise into the three-necked flask under stirring for 2 h. And [VBIm]Br (1.0 g) and 2, 2′-azobis (isobutyronitrile) (0.02 g) were added in the flask under stirring at 70 °C for 8 h. The mixture was added dropwise into the water with a vigorous stirring process, and white solid was formed. The solid was suction filtered and freeze-dried to obtain the CA modified by poly (ionic liquids) (yield: 83%).

Cellulose acetate modified by poly (ionic liquids) (2.0 g) or cellulose acetate (2.0 g) was dissolved in acetic acid (24 g) and stirred at 30 °C. Then, this solution was poured into 20 mL plastic syringe as the electrospinning fluid. Plastic syringe fixed on the slipway, with a controllable feed rate of 0.5 mL/h for electrospinning. The tip to-collector distance should be keeping in 20 cm. The potential difference of spinning machine was 20 kV (+ 15 kV and − 5 kV). Finally, the sample was vacuum-dried at 60 °C for 2 h to obtain the cellulose acetate modified by poly (ionic liquids) nano-fibrous filters (MCA-PILs-1). Similarly, MCA-PILs-2 (4.0 g CA, 0.4 g methacryloyl chloride, and 2.0 g [VBIm]Br), MCA-PILs-3 (4.0 g CA, 0.4 g methacryloyl chloride, and 3.0 g [VBIm]Br) and MCA-PILs-4 (4.0 g CA, 0.4 g methacryloyl chloride, and 4.0 g [VBIm]Br) were synthesized according to the process above, with different introduction contents of the [VBIm]Br monomer.

Characterization

The UV–Vis absorption spectra were measured on a Perkin-Elmer LAMBDA35 (USA). The chemical structures of CA, MCA-PILs-1, MCA-PILs-2, MCA-PILs-3 and MCA-PILs-4 were examined by Fourier transform infrared spectroscopy (FT-IR). FT-IR spectra were obtained using a Perkin Elmer spectrometer (PerkinElmer, Norwalk, CT, U.S.A.) in the wavenumber range from 4000 to 400 cm^{-1}. ^{1}H NMR spectra were recorded by a Bruker AVANCE 400 MHz spectrometer. The morphology and structure of fibers were examined using a JEOL JSM 7800F electron microscope (JEOL, Tokyo, Japan) with the primary electron energy of 15 kV. The chemical components of CA, MCA-PILs-1, MCA-PILs-2, MCA-PILs-3 and MCA-PILs-4 were investigated using an Oxford X-Max 50 energy dispersive X-ray spectrometer (EDS).

PM generation and efficiency measurement

The PM particles used in the experiments were obtained by burning Jade sandalwood in a glass battle. The sample was cut into a circle that was larger than the size of the glass battle in order to fix the air filter to the glass bottle mouth at an appropriate size. The bottle was inverted on the incense bottle for 5 min. PM particle number concentration was measured by a particle counter (DT-9881 M, CEM).

Antibacterial assays

Antibacterial activity of CA, MCA-PILs-1, MCA-PILs-2, MCA-PILs-3 and MCA-PILs-4 were used the following methods for the quantitative evaluation: *E. coli* (50 μL) and *S. aureus* (50 μL) were respectively transferred into 8 mL of sterile Luria-Bertani (LB) broth (10 g/L tryptone, 5 g/L yeast, 10 g/L sodium chloride). The sample (0.15 g) was sterilized under UV-A light for 1 h and then placed them in the above contain strain Luria-Bertani (LB) broth. After 12 h of incubation in a shaker-incubator (at 150 rpm and at 37 °C). All of bacterial suspensions after shaking (20 μL) were individually obtained 500 μL and then diluted to be 10^{-6} times were separately

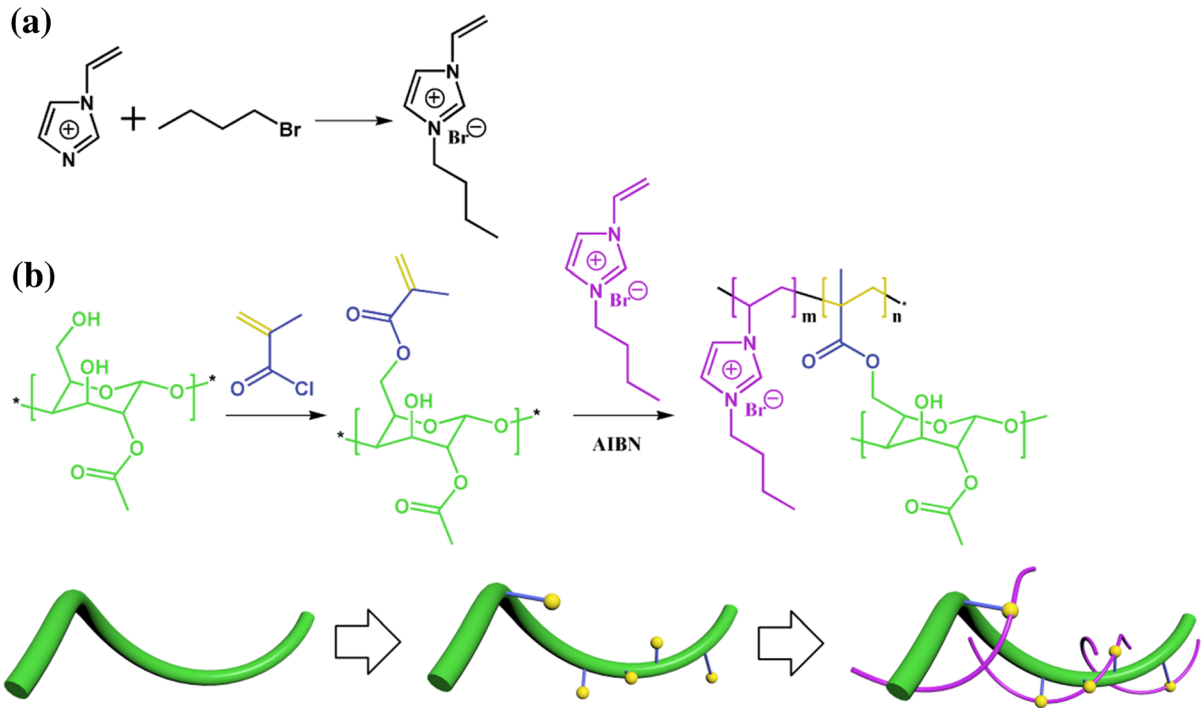

Scheme 1 **a** Synthesis route of 1-vinyl-3-butylimidazale bromide ([VBIm]Br); **b** The idea of molecular design

spread on the solid nutrient agar plates and incubated at 37 °C for 12 h. Finally, the number of the colony-forming units was calculated.

Cytotoxic activity

It is critical that air filters are of good biocompatibility, because they have the opportunity to contact human skin directly (Zarrintaj et al. 2018). In our current work, the in vitro toxicity of the prepared nano-fibrous membranes was determined by observing the growth of mouse osteoblasts in the nano-fibrous membrane through the MTT test (Li et al. 2017). First, the nano-fibrous membranes samples were soaked in deionized water for 2 days. Then, the treated nano-fibrous membranes were transferred into a 12-well culture dish and 1×10^4 cells were seeded onto every nano-fibrous membrane specimen and cultured for 24 h. Subsequently, the culture medium was removed.

The each well was added 5 mg mL^{-1} MTT solution (20 μL) and medium (180 μL) and putted them into an incubator at a temperature of 37 °C with 5% CO_2 for 4 h to form formazan. To dissolve the above formazan, we added 150 μL DMSO into each well and the plate was kept in an incubator for 2 h (at 37 °C and 5% CO_2). As the control group, 1×10^4 cells were seeded into an empty culture plate without nano-fibrous membrane. All experiments were in quintuplicate. The optical density (OD) was usually used to reflect the level of cell viability, thus the OD values of the formed formazan was quantified by using an enzyme-linked detector (BIOBASE-EL10A) at 570 nm.

Results and discussion

Synthetic mechanism of MCA-PILs nano-fibrous filters

Fibrous filter was a typical air filter, especially nano-fiber filters, which are attracting great attention (Malviya 2018). However, most spinning materials were expense and environmentally unfriendly (Jing et al. 2016). Moreover, fibrous filters were highly susceptible to bacterial pollution (Yoon et al. 2016). Therefore, molecular design technology had been applied in this work in order to solve the above problems. The idea of molecular design was shown in

the Scheme 1b. A large amount of hydroxyl groups on the surface of CA (green line) could be modified by methacryloyl chloride. Modified CA contained a large number of olefin groups (yellow sphere), which could be initiated by free radicals. Subsequently, the [VBIm]Br monomer containing olefin group was initiated by AIBN to covalently bind (blue line) CA and form polymers (purple line, poly (ionic liquids)). The poly (ionic liquids) containing a large number of positive charges could effectively destroy the phospholipid bilayer membrane of bacteria, thereby killing bacteria. In addition, the covalent bonds effectively increased the interaction between poly (ionic liquids) and CA, thus reducing the loss of functional polymers. It not only effectively improved the filtration efficiency, but also ensured no release of materials in the application process.

Characterization of MCA-PILs nano-fibrous filters

The FT-IR spectra of CA, MCA-PILs-1, MCA-PILs-2, MCA-PILs-3 and MCA-PILs-4 were shown in Fig. 1a. A strong characteristic absorption peaks at 3435 cm^{-1} could be attributed to the O–H (stretching) and N–H (stretching) vibrations, and the characteristic absorption peaks at 2962–2857 cm^{-1} were attributed to -CH_3 (stretching) and -CH_2 (stretching), and the typical vibrational absorption band of C=O at 1650 cm^{-1}. Compared with CA, the MCA-PILs appeared the characteristic peaks at 1550–1580 cm^{-1}, which was assigned to the stretching vibration of imidazolium cation. With the increase of [VBIm]Br monomer content, the intensity of the imidazolium cation absorption peaks got stronger. The peak at 1435 cm^{-1} was attributed to the C–N stretching vibrations. The ^1H NMR spectra of CA, MCA-PILs-1, MCA-PILs-2, MCA-PILs-3 and MCA-PILs-4 were shown in Fig. 1b. The ^1H NMR spectra were normalized by characteristic peaks based on CA (2.0 ppm). It was obvious that there was no characteristic peak in the ^1H NMR spectrum of CA at 7.3 ppm (this nuclear magnetic peaks position was consistent with that the [VBIm]Br monomer's peaks position in the literature). With the increase of [VBIm]Br monomer content, the characteristic peak area at 7.3 ppm increased significantly. This result suggested that the poly (ionic liquids) content in MCA-PILs was consistent with the feeding ratio of the [VBIm]Br monomer. The thermal stability of CA, MCA-PILs-1, MCA-PILs-2, MCA-PILs-3 and MCA -PILs-4 was examined by a thermogravimetric analyzer (TGA) from 0 to 700 °C (under nitrogen atmosphere). As shown in Fig. 1c, the initial thermal decomposition temperature of CA, MCA-PILs-1, MCA-PILs-2, MCA-PILs-3 and MCA-PILs-4 were around 280 °C and the rate of decomposition increased substantially in the region of 280–380 °C. After 380 °C, the weight loss stabilized again, resulting in a slow decrease to 700 °C. This result indicated that the nano-fibrous filters had good thermodynamic stability, and thermal environment would not cause weight loss of the nano-fibrous filters in practical application. It was noteworthy that the thermogravimetric curves had only one major weight loss region (280–380 °C), indicating that CA and poly (ionic liquids) had been covalently bonded to form a macromolecule.

Morphology of MCA-PILs nano-fibrous filters

The SEM images of CA, MCA-PILs-1, MCA-PILs-2, MCA-PILs-3 and MCA-PILs-4 were shown in Fig. 2, revealing the randomly arranged three-dimensional nano-fiber structures, which could be applicable for the requirement of complex structure for particle interception and air circulation. The average diameter of CA, MCA-PILs-1, MCA-PILs-2, MCA-PILs-3, MCA -PILs-4 was 680 ± 20, 519 ± 22, 446 ± 18, 410 ± 27, and 399 ± 37 nm, respectively. Obviously, the average diameter of CA fibers was bigger than the MCA-PILs fibers. With the increase of [VBIm]Br monomer content, the average diameter of MCA-PILs fibers was drastically decreased from 680 nm of the original fibers to 399 nm of the MCA-PILs-4 fibers. Besides, the diameter of fibers also became uniform. In addition the average void diameter of MCA-PILs fibers was drastically decreased and narrow distribution of fiber diameter of air filters could effectively increase the specific surface area (Fig.S2). These phenomena were mainly attributed to the introduction of poly (ionic liquids), effectively increased the conductivity of the spinning solution, thereby increasing the tensile force in electrostatic field. Small average diameter and concentrated diameter distribution were of positive significance for improving air filtration efficiency.

The EDS results of the CA, MCA-PILs-1, MCA-PILs-2, MCA-PILs-3 and MCA-PILs-4 were shown in

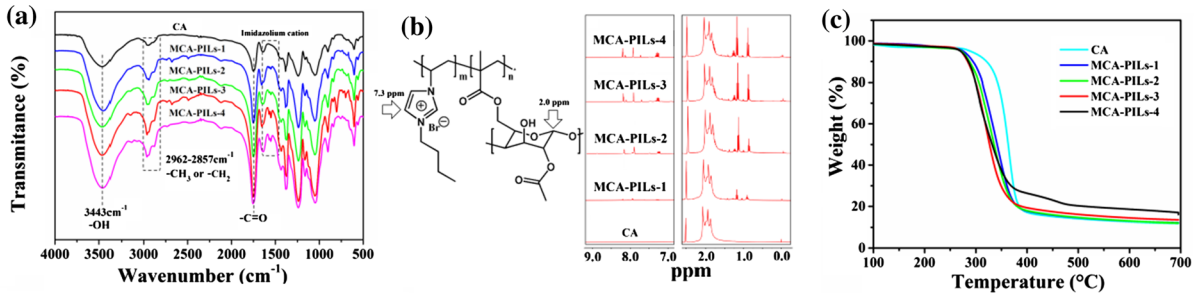

Fig. 1 **a** FT-IR spectra, **b** ^{1}H NMR spectra and **c** the TGA curves of CA, MCA-PILs-1, MCA-PILs-2, MCA-PILs-3 and MCA-PILs-4

Table 1. It confirmed the presence of C, N, O, and Br element. The content of Br element increased gradually, which was consistent with the changing trend of feeding [VBIm]Br monomers.

Filtration performance of MCA-PILs nano-fibrous filters

A simple device was used to characterize the PM removal capacity of MCA-PILs nano-fibrous filters. As shown in Fig. 3, the as-prepared nano-fibrous filters were cut into a circular shape. The filters were placed at the mouth of a glass bottle with burning wood strips. Burning wood strips would produce a large amount of white smoke, which had a lower density and would rise spontaneously (Fig. 3c). Subsequently, another clean glass bottle was placed over the device. It could be clearly found that the top glass bottle was clear and transparent. This phenomenon indicated that the nano-fibrous filters effectively reduced the diffusion of the smoke (gases containing PM particles) from the bottom glass bottle to the top glass bottle (Fig. 3d).

PM removal capacity of MCA-PILs nano-fibrous filters was systematically measured by comparing PM 2.5 and PM 10 concentrations. As shown in Fig. 3e, the CA nano-fibrous filter intercepted large particle (PM 10) effectively, while the ability to capture fine particles (PM 2.5) was poor. With the introduction of [VBIm]Br monomers, the filtration efficiency of PM 10 increased from 94.22 to 99.18% and the filtration efficiency of PM 2.5 increased from 27.14 to 91.56% (MCA-PILs-1). With the increase of [VBIm]Br monomer content, PM 2.5 and PM 10 removal capacity of MCA-PILs nano-fibrous filters were still improved (PM 10: from 99.18 to 99.65%, PM 2.5: from 96.78 to 97.94%). This phenomenon may be accounted for by two main factors: the average diameter of electrostatic spinning fibers and the charge on the surface of fibers. The removal of PM particles by filters was a dynamic process of adsorption and desorption, meaning that more opportunities for interaction and stronger interaction forces between filters and PM particles leaded to high particle removal efficiency. The small fiber average diameter and narrow fiber diameter distribution of air filters could effectively increase the specific surface area, which would increase the interaction probability between PM particles and filters. Positive charged filters could interact strongly with negatively charged PM particles, thus increasing the filtering effect of filters.

Anti-bacteria activity and cytotoxicity of MCA-PILs nano-fibrous filters

It was reported that the pollutant particles also included a variety of bacteria (Sidheswaran et al. 2012), such as *E. coli* and *S. aureus*, etc. These bacteria were responsible for the infection of air filters (Yoon et al. 2016). The bacterial-infected air filters would cause serious health problems. Therefore, it is urgently desired to develop air filters with antibacterial properties. The poly (ionic liquids) containing a large number of positive charges could effectively destroy the phospholipid bilayer membrane of bacteria, thereby killing bacteria. In addition, the covalent bonds effectively increased the interaction between poly (ionic liquids) with CA, thus reducing the loss of functional polymers. The antibacterial ability of MCA-PILs nano-fibrous filters was determined by the colony counting method (the bacteriostatic circle test could not be used to characterize their antimicrobial activity, because the MCA-PILs nano-fibrous filters did not release any antimicrobial substances).

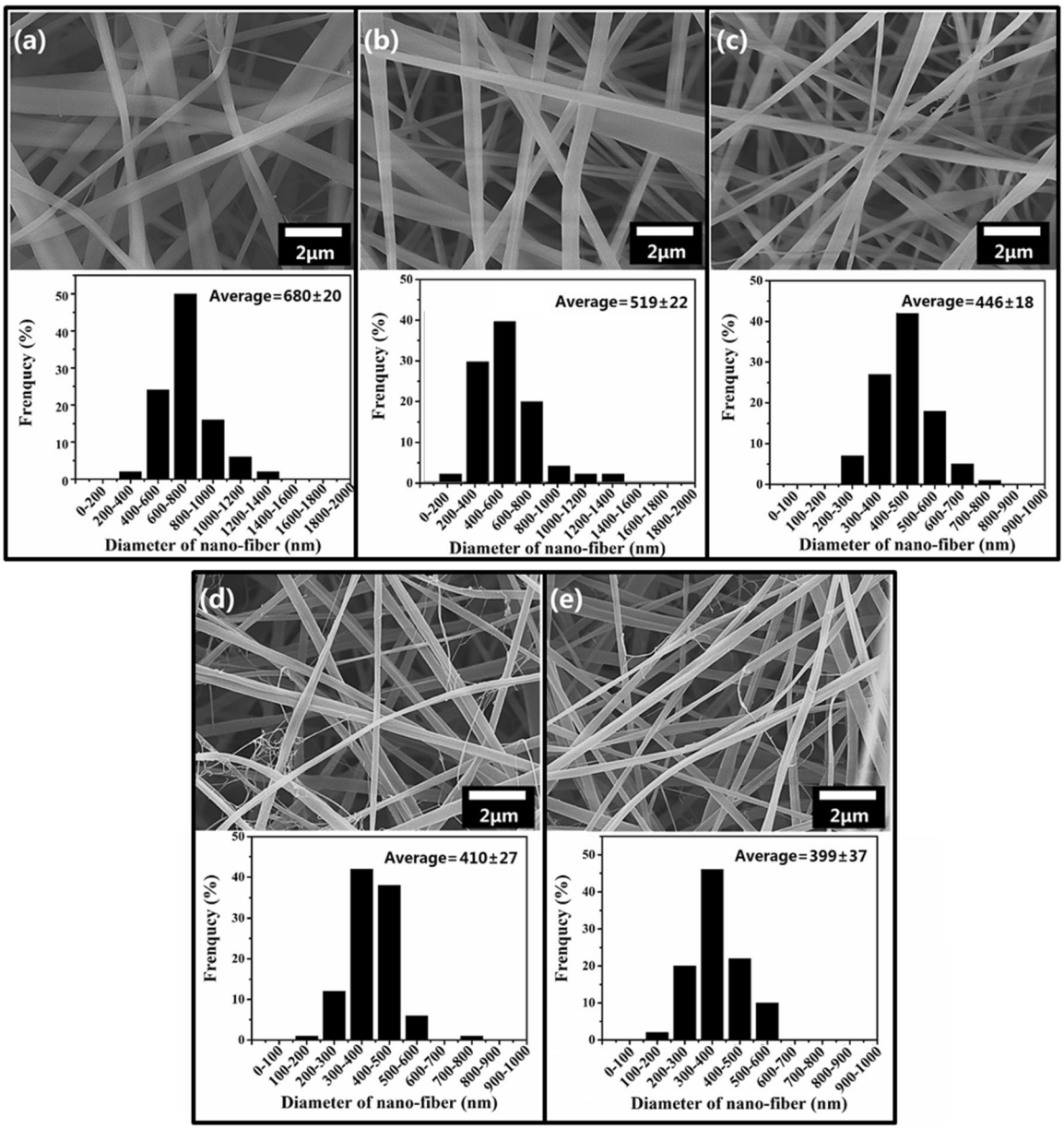

Fig. 2 SEM images of **a** CA, **b** MCA-PILs-1, **c** MCA-PILs-2, **d** MCA-PILs-3, and **e** MCA-PILs-4 nano-fibrous filter; histogram represents the fiber diameter distribution of the CA and MCA-PILs nano-fibrous filters

Table 1 The EDS data of C, O, N, Br element content in the the CA and MCA-PILs nano-fibrous filters

Sample/element (wt%)	CA	MCA-PILs-1	MCA-PILs-2	MCA-PILs-3	MCA-PILs-4
C	72.77	72.14	79.23	74.60	74.37
O	27.23	26.49	17.98	17.17	16.86
N	0.00	0.74	1.66	5.04	4.33
Br	0.00	0.64	1.13	3.18	4.46
Total	100.00	100.00	100.00	100.00	100.00

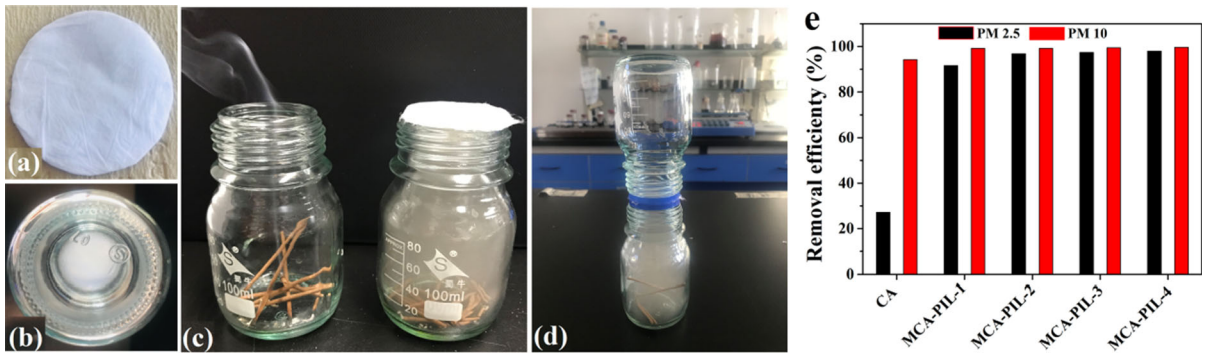

Fig. 3 **a** The as-prepared nano-fibrous filter; **b** top view of the nano-fibrous filter covering the mouth of the bottle; **c** the glass bottle without nano-fibrous filter on the left, the glass bottle with nano-fibrous filter on the right; **d** the as-prepared nano-fibrous filter is used for blocking the diffusion of smoke from the bottom bottle to the outer space; **e** the removal efficiencies by the CA and MCA-PILs nano-fibrous filters for PM 2.5 and PM 10

The photographs of agar plates were shown in Fig. 4a and b. The MCA-PILs nano-fibrous filters exhibited obvious antibacterial activities against both *E. coli* and *S. aureus*, while CA nano-fibrous filters had no significant antibacterial activity against all strains. It is worth noting that there was an obvious correlation between the degree of antibacterial activity and the [VBIm]Br monomer content of the nano-fibrous filters. With the increase of [VBIm]Br monomer content, antibacterial activity of MCA-PILs nano-fibrous filters improved significantly. Notably, 100% of the bacteria were killed after contacting with MCA-PILs-4 for 24 h.

The antibacterial properties of the MCA-PILs nano-fibrous filters furthermore were confirmed by OD data of bacterial suspension after 24 h incubation growth using OD600 measurement. As shown in Fig. 4c and d, the *E. coli* and *S. aureus* suspension for CA nano-fibrous filters were opaque and turbid, and the OD data was high, indicating that the microbial activity had not been inhibited in CA nano-fibrous filters system. With the introduction of [VBIm]Br monomer, OD data of *E. coli* and *S. aureus* suspension obviously reduced, and the transparency increased significantly. It is noteworthy that MCA-PILs nano-fibrous filters inhibited *S. aureus* activity at lower [VBIm]Br content (MCA-PILs-1), and inhibition ability on *E. coli* had the same trend. MCA-PILs-4 had the best ability to inhibit microbial activity, which was in accordance with the results of the colony counting method.

Because air filters had the opportunity to contact human skin directly, the toxicity of MCA-PILs nano-fibrous filters was an important property in practical applications As shown in Fig. S1, the MCA-PILs nano-fibrous filters didn't significantly influence the cell growth, implying that the MCA-PILs nano-fibrous filters did not release harmful substances, and it was non-cytotoxic for MC3T3-E1 cells. To assess the cytotoxicity of MCA-PILs-n nano-fibrous membranes, the toxicity in vitro of all the MCA-PILs-n nano-fibrous membranes were evaluated against mouse osteoblasts (MC3T3-E1) by the MTT test.

Recycling experiment of MCA-PILs nano-fibrous filters

Recycling of air filters was important in practical application. It effectively reduced the using cost of the air filters and the loss of resources. In order to prove the recyclability of MCA-PILs nano-fibrous filters, the used CA, MCA-PILs-1, MCA-PILs-2, MCA-PILs-3 and MCA-PILs-4 nano-fibrous filters were sterilized in a sterilization high temperature sterilizer at 120 °C for 40 min and then immerse them in ultra-pure water for 24 h. Finally, vacuum dried them at 60 °C for 120 min. The above process was repeated 20 times. For the antibacterial experiment, the MCA-PILs nano-fibrous filters still exhibited obvious antibacterial activities against both *E. coli* and *S. aureus*, while CA nano-fibrous filters had no significant antibacterial activity against all strains (Fig. 5a and b). As shown in Fig. 5c and d, with the increase of [VBIm]Br content, the number of colonies decreased, and the removal efficiency of the bacteria increased. The antibacterial efficiency of the MCA-PILs nano-fibrous filters still

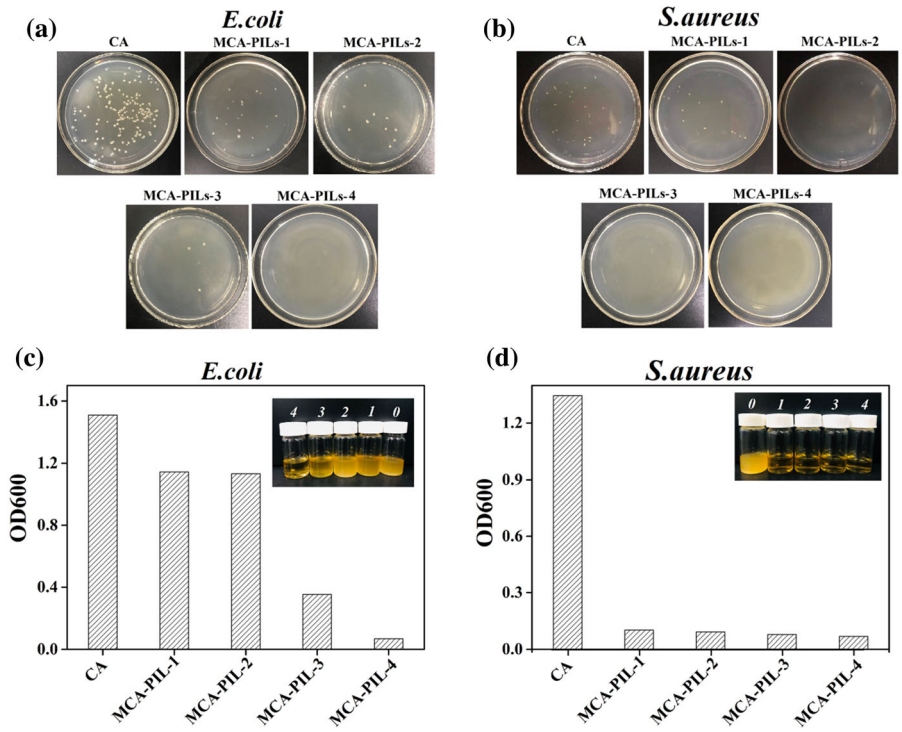

Fig. 4 Photographs of bacterial colonies of **a** *S. aureus* and **b** *E. coli* treated with the CA and MCA-PILs nano-fibrous filters; OD data of **c** *E. coli* and **d** *S. aureus* suspensions, the inserted photographs are their corresponding bacterial suspension after 24 h incubation

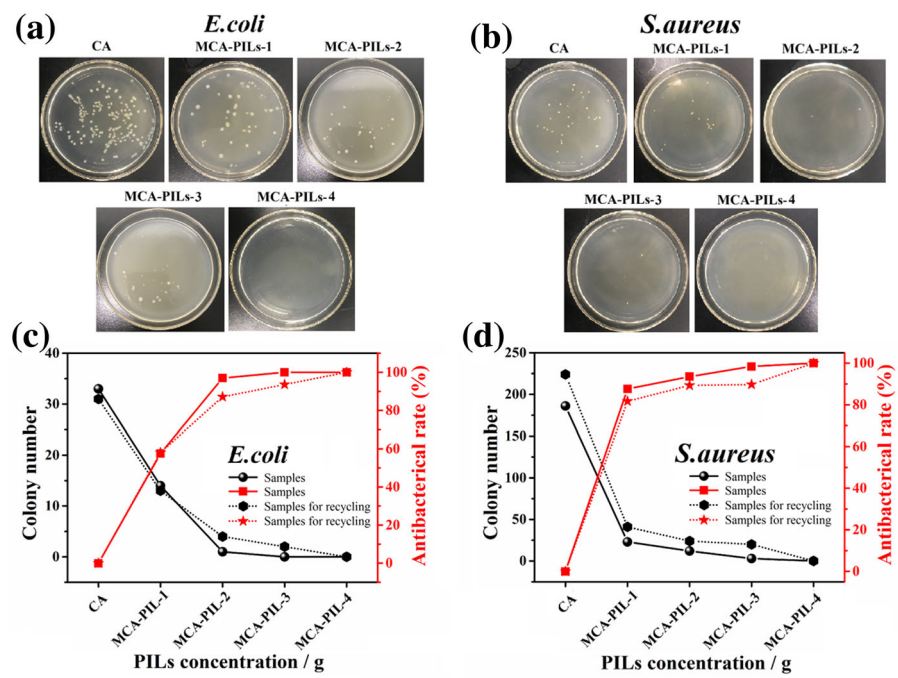

Fig. 5 Photographs of the repeated antibacterial colonies of **a** *S. aureus* and **b** *E. coli* treated with the CA and MCA-PILs nano-fibrous filters; the line chart graphs are the colony number and antibacterial rate of **c** *S. aureus* and **d** *E. coli* treated with the CA and MCA-PILs nano-fibrous filters

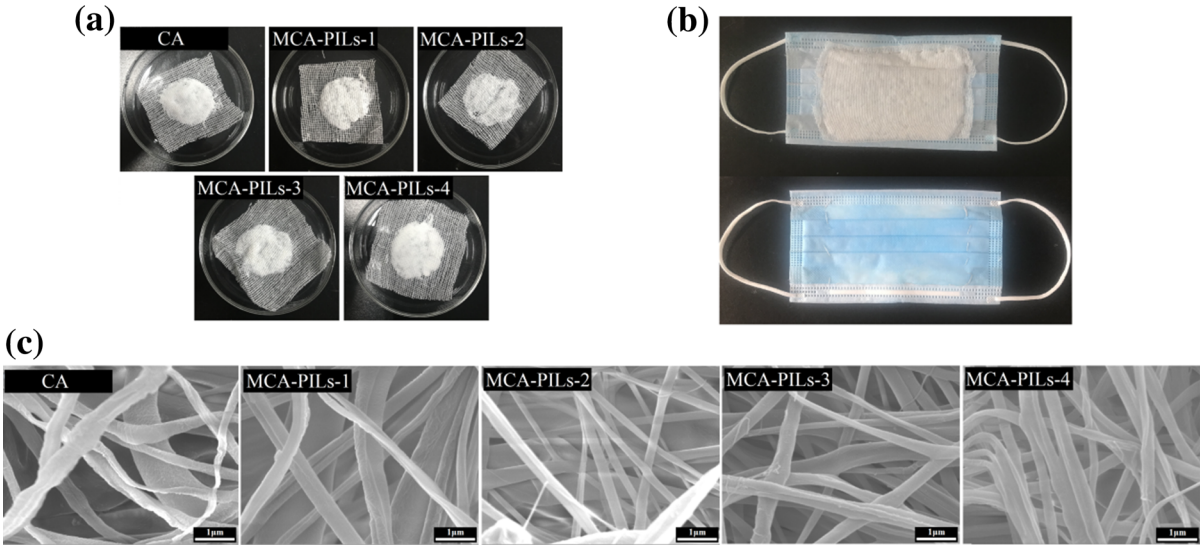

Fig. 6 **a** Picture of the fiber solution dripping onto the gauze; **b** picture of the fiber solution dripping onto the gauze and sewing it on the commercial breathing mask; **c** SEM images of the fiber solution dripping onto the gauze

maintained after recycling. The results suggested that the MCA-PILs nano-fibrous filters had good stability and could be recycled. The prolonged high temperature (120 °C), ultra-pure water immersion and ultraviolet irradiation did not decrease antimicrobial activity of MCA-PILs nano-fibrous filters. This result was mainly attributed to the chemical bond connection between poly (ionic liquids) and CA, which was beneficial to reduce the loss of the poly (ionic liquids).

Practical application of MCA-PILs nano-fibrous filters

The main limitation of electrospinning nano-fibrous filters in practical application was that the fiber felt was too dense, which was not conducive to human normal breathing. Therefore, the application of electrospinning nano-fibrous filters as fillers in commercial mask filters was of great significance. The MCA-PILs nano-fibrous filters were disintegrated with a Deflaker in deionized water. Dispersed MCA-PILs nano-fibrous filters were dripped onto the gauze. As shown in Fig. 6a, the MCA-PILs nano-fibrous filters were easily processed to the surface of the gauze. Dispersed MCA-PILs nano-fibrous filters were white flocculent, much like cotton. Furthermore, the MCA-PILs nano-fibrous filters were easily processed into commercial masks (Fig. 6b). The morphologies of dispersed MCA-PILs nano-fibrous filters were shown in Fig. 6c. It was observed that the CA, MCA-PILs-1,MCA-PILs-2, MCA-PILs-3 and MCA-PILs-4 nano-fibrous filters all maintained their original filamentous morphologies after dispersion and processing.

Conclusions

In this work, we designed a simple method to synthesize a novel air filter, which composed of cellulose acetate and poly (ionic liquids). The introduction of poly (ionic liquids) effectively reduced the diameter of fibers and thus obtains nano-fibrous filters. The removal rate of PM 10 and PM 2.5 particle by the filters reached 99.65% and 97.94%, respectively. Furthermore, the filters exhibited excellent antibacterial properties against *E. coli* and *S. aureus*, and no obvious cytotoxicity was observed in vitro culturing cell. After multiple recycling, the filters still maintain excellent antimicrobial properties and fibrous morphology. This result is mainly attributed to the covalent bonds between cellulose acetate and poly (ionic liquids). This is a novel strategy to prepare high-quality air filters, which have great potential applications in air purification.

Acknowledgments This study was supported by National Natural Science Foundation of China (Nos. 31800498, 31770635 and 31470604).

Compliance with ethical standards

Conflict of interest There are no conflicts to declare.

References

Arca HC, Mosquera-Giraldo LI, Bi V, Xu D, Taylor LS, Edgar KJ (2018) Pharmaceutical applications of cellulose ethers and cellulose ether esters. Biomacromol 19(7):2351–2376. https://doi.org/10.1021/acs.biomac.8b00517

Bazbouz MB, Taylor M, Baker D, Ries ME, Goswami P (2019) Dry-jet wet electrospinning of native cellulose microfibers with macroporous structures from ionic liquids. J Appl Polym Sci. https://doi.org/10.1002/app.47153

Brook RD, Rajagopalan S, Pope CA 3rd, Brook JR, Bhatnagar A, Diez-Roux AV, Holguin F, Hong Y, Luepker RV, Mittleman MA, Peters A, Siscovick D, Smith SC Jr, Whitsel L, Kaufman JDE (2010) American Heart Association Council on, C.o.t.K.i.C.D. Prevention, P.A. Council on Nutrition and Metabolism. Particulate matter air pollution and cardiovascular disease: an update to the scientific statement from the american heart association. Circulation 121(21):2331–2378. https://doi.org/10.1161/CIR.0b013e3181dbece1

Cheng Y-Y, Du C-H, Wu C-J, Sun K-X, Chi N-P (2018) Improving the hydrophilic and antifouling properties of poly(vinyl chloride) membranes by atom transfer radical polymerization grafting of poly(ionic liquid) brushes. Polym Adv Technol 29(1):623–631. https://doi.org/10.1002/pat.4172

De France KJ, Babi M, Vapaavuori J, Hoare T, Moran-Mirabal J, Cranston ED (2019) 2.5D hierarchical structuring of nanocomposite hydrogel films containing cellulose nanocrystals. ACS Appl Mater Interfaces 11(6):6325–6335. https://doi.org/10.1021/acsami.8b16232

Elshaarawy RFM, Mustafa FHA, Sofy AR, Hmed AA, Janiak C (2019) A new synthetic antifouling coatings integrated novel aminothiazole-functionalized ionic liquids motifs with enhanced antibacterial performance. J Environ Chem Eng. https://doi.org/10.1016/j.jece.2018.11.044

Fan X, Wang Y, Kong L, Fu X, Zheng M, Liu T, Zhong W-H, Pan S (2018) A nanoprotein-functionalized hierarchical composite air filter. ACS Sustain Chem Eng 6(9):11606–11613. https://doi.org/10.1021/acssuschemeng.8b01827

Fang H, Wang J, Li L, Xu L, Wu Y, Wang Y, Fei X, Tian J, Li Y (2019) A novel high-strength poly(ionic liquid)/PVA hydrogel dressing for antibacterial applications. Chem Eng J 365:153–164. https://doi.org/10.1016/j.cej.2019.02.030

Gu GQ, Han CB, Lu CX, He C, Jiang T, Gao ZL, Li CJ, Wang ZL (2017) Triboelectric nanogenerator enhanced nanofiber air filters for efficient particulate matter removal. ACS Nano 11(6):6211–6217. https://doi.org/10.1021/acsnano.7b02321

Han H, Zhu J, De-Qun W, Li F-X, Wang X-L, Jian-Yong Yu, Qin X-H (2019) Inherent guanidine nanogels with durable antibacterial and bacterially antiadhesive properties. Adv Funct Mater. https://doi.org/10.1002/adfm.201806594

Hu J, Huang L, Chen M, Liao H, Zhang H, Wang S, Zhang Q, Ying Q (2017) Premature mortality attributable to particulate matter in China: source contributions and responses to reductions. Environ Sci Technol 51(17):9950–9959. https://doi.org/10.1021/acs.est.7b03193

Jiang F, Kittle JD, Tan X, Esker AR, Roman M (2013) Effects of sulfate groups on the adsorption and activity of cellulases on cellulose substrates. Langmuir ACS J Surf Colloids 29(10):3280–3291. https://doi.org/10.1021/la3040193

Jing L, Shim K, Toe CY, Fang T, Zhao C, Amal R, Sun KN, Kim JH, Ng YH (2016) Electrospun polyacrylonitrile-ionic liquid nanofibers for superior $PM_{2.5}$ capture capacity. ACS Appl Mater Interfaces 8(11):7030–7036. https://doi.org/10.1021/acsami.5b12313

Khalid B, Bai X, Wei H, Huang Y, Wu H, Cui Y (2017) Direct blow-spinning of nanofibers on a window screen for highly efficient $PM_{2.5}$ removal. Nano Lett 17(2):1140–1148. https://doi.org/10.1021/acs.nanolett.6b04771

Li X, Anderson P, Jhong H-RM, Paster M, Stubbins JF, Kenis PJA (2016) Greenhouse gas emissions, energy efficiency, and cost of synthetic fuel production using electrochemical CO_2 conversion and the Fischer–Tropsch process. Energy Fuels 30(7):5980–5989. https://doi.org/10.1021/acs.energyfuels.6b00665

Li Q, Xie S, Serem WK, Naik MT, Liu L, Yuan JS (2017) Quality carbon fibers from fractionated lignin. Green Chem 19(7):1628–1634. https://doi.org/10.1039/c6gc03555h

Li X, Wang XX, Yue TT, Xu Y, Zhao ML, Yu M, Ramakrishna S, Long YZ (2019) Waterproof-breathable PTFE nano- and microfiber membrane as high efficiency $PM_{2.5}$ filter. Polymers (Basel). https://doi.org/10.3390/polym11040590

Liu K, Liu C, Hsu PC, Xu J, Kong B, Wu T, Zhang R, Zhou G, Huang W, Sun J, Cui Y (2018) Core-shell nanofibrous materials with high particulate matter removal efficiencies and thermally triggered flame retardant properties. ACS Cent Sci 4(7):894–898. https://doi.org/10.1021/acscentsci.8b00285

Lopez AM, Cowan MG, Gin DL, Noble RD (2018) Phosphonium-based poly(ionic liquid)/ionic liquid ion gel membranes: influence of structure and ionic liquid loading on ion conductivity and light gas separation performance. J Chem Eng Data 63(5):1154–1162. https://doi.org/10.1021/acs.jced.7b00541

Lu Z, Su Z, Song S, Zhao Y, Ma S, Zhang M (2017) Toward high-performance fibrillated cellulose-based air filter via constructing spider-web-like structure with the aid of TBA during freeze-drying process. Cellulose 25(1):619–629. https://doi.org/10.1007/s10570-017-1561-x

Ma S, Zhang M, Nie J, Yang B, Song S, Lu P (2018) Multifunctional cellulose-based air filters with high loadings of metal–organic frameworks prepared by in situ growth method for gas adsorption and antibacterial applications. Cellulose 25(10):5999–6010. https://doi.org/10.1007/s10570-018-1982-1

Ma S, Zhang M, Nie J, Tan J, Yang B, Song S (2019) Design of double-component metal–organic framework air filters with $PM_{2.5}$ capture, gas adsorption and antibacterial capacities. Carbohydr Polym 203:415–422. https://doi.org/10.1016/j.carbpol.2018.09.039

Malviya RM (2018) Nano-fiber filters for automotive applications 1. https://doi.org/10.4271/2018-28-0041

Napso S, Rein DM, Fu Z, Radulescu A, Cohen Y (2018) Structural analysis of cellulose-coated oil-in-water emulsions fabricated from molecular solution. Langmuir ACS J Surf Colloids 34(30):8857–8865. https://doi.org/10.1021/acs.langmuir.8b01325

Osaka Y, Iwai K, Tsujiguchi T, Kodama A, Li X, Huang H (2019) Basic study on exhaust gas purification by utilizing plasma assisted MnO_2 filter for zero-emission diesel. Sep Purif Technol 215:108–114. https://doi.org/10.1016/j.seppur.2018.12.077

Raaschou-Nielsen O, Andersen ZJ, Beelen R, Samoli E, Stafoggia M, Weinmayr G, Hoffmann B, Fischer P, Nieuwenhuijsen MJ, Brunekreef B, Xun WW, Katsouyanni K, Dimakopoulou K, Sommar J, Forsberg B, Modig L, Oudin A, Oftedal B, Schwarze PE, Nafstad P, De Faire U, Pedersen NL, Östenson C-G, Fratiglioni L, Penell J, Korek M, Pershagen G, Eriksen KT, Sørensen M, Tjønneland A, Ellermann T, Eeftens M, Peeters PH, Meliefste K, Wang M, Bueno-de-Mesquita B, Key TJ, de Hoogh K, Concin H, Nagel G, Vilier A, Grioni S, Krogh V, Tsai M-Y, Ricceri F, Sacerdote C, Galassi C, Migliore E, Ranzi A, Cesaroni G, Badaloni C, Forastiere F, Tamayo I, Amiano P, Dorronsoro M, Trichopoulou A, Bamia C, Vineis P, Hoek G (2013) Air pollution and lung cancer incidence in 17 European cohorts: prospective analyses from the European Study of Cohorts for Air Pollution Effects (ESCAPE). Lancet Oncol 14(9):813–822. https://doi.org/10.1016/s1470-2045(13)70279-1

Seo JM, Arumugam GK, Khan S, Heiden PA (2009) Comparison of the effects of an ionic liquid and triethylbenzylammonium chloride on the properties of electrospun fibers, 1—poly(lactic acid). Macromol Mater Eng 294(1):35–44. https://doi.org/10.1002/mame.200800198

Shanmugam K, Gadhamshetty V, Yadav P, Athanassiadis D, Tysklind M, Upadhyayula VKK (2019) Advanced high strength steel and carbon fiber reinforced polymer composite body in white for passenger cars: environmental performance and sustainable return on investment under different propulsion modes. ACS Sustain Chem Eng 7:4951–4963

Sidheswaran MA, Destaillats H, Sullivan DP, Cohn S, Fisk WJ (2012) Energy efficient indoor VOC air cleaning with activated carbon fiber (ACF) filters. Build Environ 47:357–367. https://doi.org/10.1016/j.buildenv.2011.07.002

Sobhanadhas S, Kesavan LL, Lastusaari M, Fardim P (2019) Layered double hydroxide-cellulose hybrid beads: a novel catalyst for topochemical grafting of pulp fibers. ACS Omega 4(1):320–330. https://doi.org/10.1021/acsomega.8b03061

Song N, Hou X, Chen L, Cui S, Shi L, Ding P (2017) A green plastic constructed from cellulose and functionalized graphene with high thermal conductivity. ACS Appl Mater Interfaces 9(21):17914–17922. https://doi.org/10.1021/acsami.7b02675

Tan NPB, Paclijan SS, Ali HNM, Hallazgo CMJS, Lopez CJF, Ebora YC (2019) Solution blow spinning (SBS) nanofibers for composite air filter masks. ACS Appl Nano Mater 2(4):2475–2483. https://doi.org/10.1021/acsanm.9b00207

Tort S, Acarturk F (2016) Preparation and characterization of electrospun nanofibers containing glutamine. Carbohydr Polym 152:802–814. https://doi.org/10.1016/j.carbpol.2016.07.028

Wang N, Zhu Z, Sheng J, Al-Deyab SS, Yu J, Ding B (2014) Superamphiphobic nanofibrous membranes for effective filtration of fine particles. J Colloid Interface Sci 428:41–48. https://doi.org/10.1016/j.jcis.2014.04.026

Wang Z, Pan Z, Wang J, Zhao R (2016) A novel hierarchical structured poly(lactic acid)/titania fibrous membrane with excellent antibacterial activity and air filtration performance. J Nanomater 2016:1–17. https://doi.org/10.1155/2016/6272983

Wang A, Fan R, Zhou X, Hao S, Zheng X, Yang Y (2018a) Hot-pressing method to prepare imidazole-based Zn(II) metal-organic complexes coatings for highly efficient air filtration. ACS Appl Mater Interfaces 10(11):9744–9755. https://doi.org/10.1021/acsami.8b01287

Wang Z, Yan F, Pei H, Li J, Cui Z, He B (2018b) Antibacterial and environmentally friendly chitosan/polyvinyl alcohol blend membranes for air filtration. Carbohydr Polym 198:241–248. https://doi.org/10.1016/j.carbpol.2018.06.090

Wang K, Wang J, Li L, Xu L, Feng N, Wang Y, Fei X, Tian J, Li Y (2019) Synthesis of a novel anti-freezing, non-drying antibacterial hydrogel dressing by one-pot method. Chem Eng J 372:216–225. https://doi.org/10.1016/j.cej.2019.04.107

Xiong Z-C, Yang R-L, Zhu Y-J, Chen F-F, Dong L-Y (2017) Flexible hydroxyapatite ultralong nanowire-based paper for highly efficient and multifunctional air filtration. J Mater Chem A 5(33):17482–17491. https://doi.org/10.1039/c7ta03870d

Xue J, Wu T, Dai Y, Xia Y (2019) Electrospinning and electrospun nanofibers: methods, materials, and applications. Chem Rev 119(8):5298–5415. https://doi.org/10.1021/acs.chemrev.8b00593

Yang J, Xiong S, Qu T, Zhang Y, He X, Guo X, Zhao Q, Braun S, Chen J, Xu J, Li Y, Liu X, Duan C, Tang J, Fahlman M, Bao Q (2019) Extremely low-cost and green cellulose passivating perovskites for stable and high-performance solar cells. ACS Appl Mater Interfaces 11(14):13491–13498. https://doi.org/10.1021/acsami.9b01740

Yoon Y, Kim S, Ahn KH, Ko KB, Kim KS (2016) Fabrication and characterization of micro-porous cellulose filters for indoor air quality control. Environ Technol 37(6):703–712. https://doi.org/10.1080/09593330.2015.1078416

Zarrintaj P, Manouchehri S, Ahmadi Z, Saeb MR, Urbanska AM, Kaplan DL, Mozafari M (2018) Agarose-based biomaterials for tissue engineering. Carbohydr Polym 187:66–84. https://doi.org/10.1016/j.carbpol.2018.01.060

Zhang S, Tang N, Cao L, Yin X, Yu J, Ding B (2016) Highly integrated polysulfone/polyacrylonitrile/polyamide-6 air filter for multilevel physical sieving airborne particles. ACS Appl Mater Interfaces 8(42):29062–29072. https://doi.org/10.1021/acsami.6b10094

Zhang Q, Li Q, Young TM, Harper DP, Wang AS (2019a) A novel method for fabricating an electrospun poly(vinyl alcohol)/cellulose nanocrystals composite nanofibrous filter with low air resistance for high-efficiency filtration of particulate matter. ACS Sustain Chem Eng. https://doi.org/10.1021/acssuschemeng.9b00605

Zhang S, Rind NA, Tang N, Liu H, Yin X, Yu J, Ding B (2019b) Electrospun nanofibers for air filtration. William Andrew Publishing, Norwich, pp 365–389. https://doi.org/10.1016/b978-0-323-51270-1.00012-1

Zhu M, Han J, Wang F, Shao W, Xiong R, Zhang Q, Pan H, Yang Y, Samal SK, Zhang F, Huang C (2017) Electrospun nanofibers membranes for effective air filtration. Macromol Mater Eng 302(1):1600353. https://doi.org/10.1002/mame.201600353

Zhu F, Yan F, Wang Y, Zhang Z, Li C, Dong Y (2018a) Inhibition of $PM_{2.5}$ emission from the combustion of waste materials. Energy Fuels 32(10):10941–10950. https://doi.org/10.1021/acs.energyfuels.8b01231

Zhu M, Hua D, Pan H, Wang F, Manshian B, Soenen SJ, Xiong R, Huang C (2018b) Green electrospun and crosslinked poly(vinyl alcohol)/poly(acrylic acid) composite membranes for antibacterial effective air filtration. J Colloid Interface Sci 511:411–423. https://doi.org/10.1016/j.jcis.2017.09.101

Zhu M, Xiong R, Huang C (2019) Bio-based and photocrosslinked electrospun antibacterial nanofibrous membranes for air filtration. Carbohydr Polym 205:55–62. https://doi.org/10.1016/j.carbpol.2018.09.075